

flowfield and that temperatures could be hazardous to the airplane. The test program was therefore extended to investigate changes in JBD design which might improve the environment. The three configurations described previously, selected as requiring minimum modifications to existing deflectors, were tested. The results of these tests are shown in Fig. 18, with results from the standard deflector included for comparison.

From Fig. 18 it can be seen that these tests successfully demonstrated a JBD design that will prevent any hot gas from reaching the airplane. It can also be seen that modifications which were beneficial in some locations were detrimental in other locations, and that the momentum balance is not adequate to determine the effects of modifications. The fence was expected to turn the forward flow outboard, and (to an extent) it was successful. However, the temperature at the top of the vertical tail shows that the fence also augmented the upward flow. Similarly, reducing the JBD angle to 45° was expected to lower all temperatures on the airplane, but it increased the temperature at the engine inlet.

These test results were valuable in the F-111B program and are generally applicable for situations that duplicate the F-111B nozzle spacing, height above the deck, and nozzle inclination. In any other case, the uncertainties in analysis as demonstrated in this test are such that data from exact models should be obtained.

References

- ¹ Fleming, W. A., "Characteristics of a hot jet discharged from a jet-propulsion engine," NACA RM E6L27a (1946).
- ² Sloop, J. L. and Morrell, G., "Temperature survey in the wake of two closely located parallel jets," NACA TM E9L21 (1950).
- ³ Farmer, J. E., Stepka, F. S., and Garrett, F. B., "Temperature and pressure distribution in dual parallel jets impinging on the ground from a turbojet engine," NACA RM E9L01 (1950).
- ⁴ "Nondimensional characteristics of free and deflected supersonic jets exhausting into quiescent air," Naval Air Development Center Rept. NADC-ED-5401 (1954).
- ⁵ *Aero-Space Applied Thermodynamics Manual* (Society of Automotive Engineers Inc., New York, 1962), p. C-61.

Nozzles for Jet-Lift V/STOL Aircraft

J. A. C. KENTFIELD*

Curtiss-Wright Corporation, Wood-Ridge, N. J.

Several types of nozzles for lift and lift/cruise engines are reviewed. Model test data are presented for two types of lift-engine nozzles, one of the short nonvectoring plug type, the other a simple, hemispherical-plug, vectoring nozzle. It was found that the thrust and discharge coefficients obtained with the simple vectoring nozzle were substantially independent of flow-deflection angle. Results of a theoretical analysis are presented which show that attempts to shorten and lighten lift-engine nozzles by eliminating whirl-removing surfaces may incur severe performance penalties. An oblique-joint, elliptical shape nozzle for vectoring lift/cruise engine thrust is described and test data obtained with homogeneous flow are presented. A theoretical analysis was made of the causes of performance loss with non-homogeneous flow. It was concluded that when a nozzle of this type is employed on a turbofan engine use should be made of an upstream flow mixer, or separate channels to the nozzle exit, if excessive losses are to be avoided in the vectored mode.

Nomenclature

B	= bypass ratio
C_D	= discharge coefficient; (actual mass flow)/(ideal mass flow for corresponding λ)
C_T	= thrust coefficient; (actual thrust for actual mass flow)/(ideal thrust for the same mass flow)
D	= maximum engine diameter or major axis of elliptic section
d	= minor axis of elliptic section
F	= thrust augmentation ratio

M	= Mach number
n	= number of oblique joints
P	= static pressure
P_o	= total pressure
P_∞	= ambient pressure
r	= radius
X	= downward projection or axial length of nozzle
α	= ratio; (enthalpy of gas generator flow)/(enthalpy of fan flow)
β	= actual flow-deflection angle
β_g	= nominal flow-deflection angle based on nozzle geometry
γ	= ratio of specific heats
Δ	= finite increment
θ	= inclination angle of oblique joint
λ	= nozzle pressure ratio
ρ	= density
φ	= flow-discharge angle of truncated plug nozzle
Φ	= whirl angle

Presented at the AIAA Second Propulsion Joint Specialist Conference, Colorado Springs, Colo., June 13-17, 1966 (not preprinted); received October 5, 1966; revision received March 30, 1967. The author wishes to thank the management of the Curtiss-Wright Corporation for permitting the publication of this paper. The efforts of the author's colleagues at the Wright Aeronautical Division who carried out the programming of the flow mixing analysis and assisted in other ways are gratefully acknowledged. The Fluidyne Engineering Corporation of Minneapolis, Minn. obtained the experimental results presented herein under contract from the Curtiss-Wright Corporation. [4.01]

* Project Engineer, Wright Aeronautical Division; now Lecturer, Mechanical Engineering Department, Imperial College, University of London.

Subscripts

(AXIAL)	= axial component
b	= pertaining to base area of truncated plug nozzle
C	= cold (fan) flow of a turbofan engine
EQV	= circular cross section of equivalent area

EXT	= nozzle exit
H	= hot (gas generator) flow of a turbofan engine
i	= inner surface
j	= pertaining to outer surface of exhaust jet
M	= fully mixed flow of a turbofan engine
MAX	= maximum value
o	= outer surface
(RESUL)	= resultant (vector sum of axial and whirl components)
(WHIRL)	= whirl component
1, 2	= reference stations

Introduction

THE increasing attention given to vertical takeoff aircraft has resulted in the study of numerous aircraft/power-plant configurations. Arrangements of powerplants already in use in such aircraft include remote fan-in-wing designs to augment cruise engine thrust for lift purposes, batteries of specialized lift engines divorced from the cruise power units, tilting and also thrust vectoring lift/cruise engines etc. Various combinations of these schemes have either been tried or proposed.

Available literature on the subject of lift, and lift/cruise, engine nozzles and their installation deals mainly with the effect of ground proximity on nozzle performance¹ and the relationship, for various aircraft configurations between the location of the nozzle exits and the lift performance in and out of ground effect.² Other works show how ground pressure and temperature signatures can be reduced by use of nozzle exit shapes which encourage rapid mixing of the exhaust gases with the ambient air.³ A recent paper⁴ describes experiments covering the effect of horizontal airflow, such as exists during transition, on the performance of lift-engine thrust nozzles. Results of some tests showing the effect of turbine residual whirl on nozzle thrust coefficient are also included.

In this paper attention is focused on the design and static performance of thrust nozzles for lift and lift/cruise turbojet and turbofan engines. Because of the vast number of conceivable individual nozzle designs, an attempt has been made to categorize some of the more basic concepts into three broad groups: nonvectoring nozzles for lift engines,

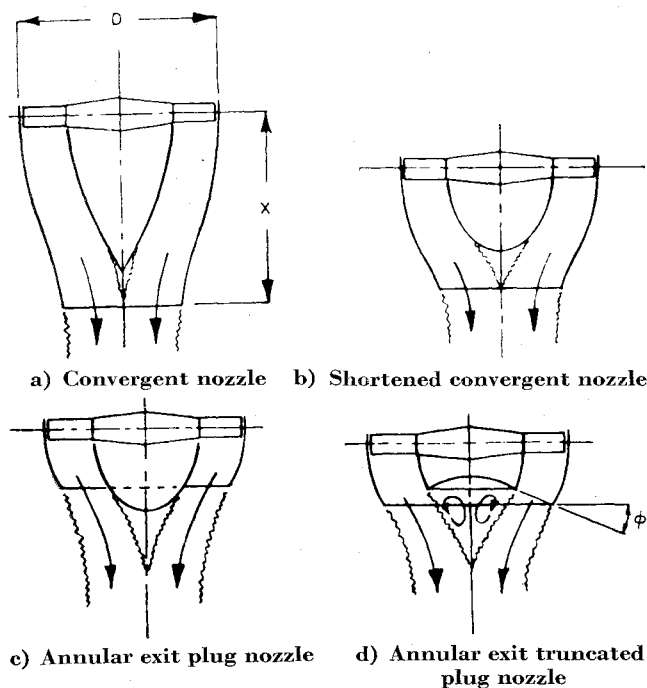


Fig. 1 Nonvectoring nozzles for lift engines.

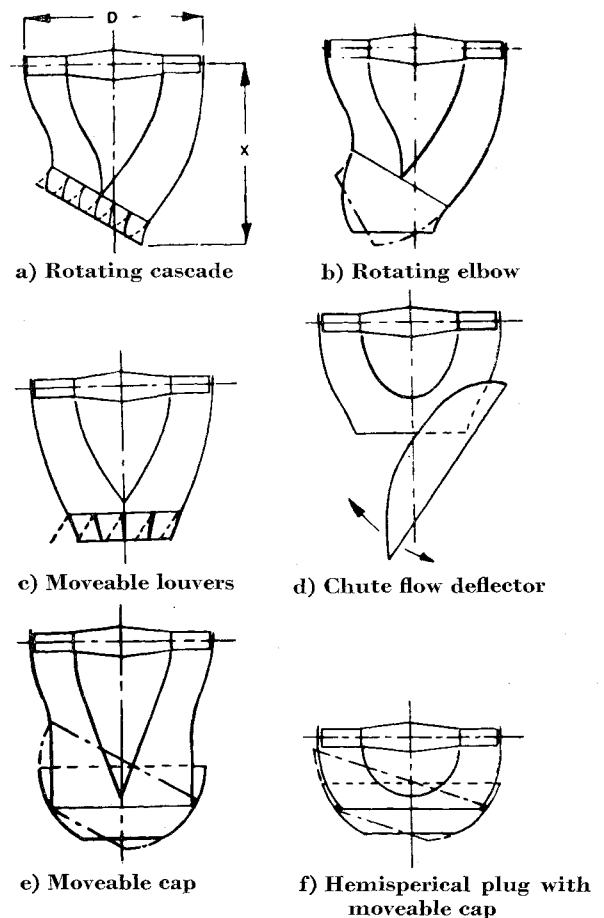


Fig. 2 Vectoring nozzles for lift engines.

vectoring nozzles for lift engines, and vectoring nozzles for lift/cruise engines.

Nozzle Concepts for Lift Engines

Four types of nonvectoring lift engine nozzles are illustrated in Fig. 1. The design in Fig. 1a is merely the type of convergent nozzle commonly used for propulsion purposes. The prime objection to such a concept is the appreciable axial length of the nozzle. Figure 1b is a modified version of Fig. 1a incorporating a shortened centerbody resulting in a reduction of the over-all length of the nozzle.

Nozzle length can be reduced still further by arranging the exit to form an annulus around the centerbody as illustrated in Fig. 1c. Truncation of the centerbody leads to the design shown in Fig. 1d. In general the length and weight of a nozzle of this type will be minimized when the inclination angle ϕ is as small as possible. However, it has been established by others⁵ that when ϕ is approximately zero a substantial base drag can be developed because of suction on the truncated end face of the centerbody. The experimental determination of the minimum acceptable value of ϕ consistent with a good thrust coefficient was the objective of a systematic series of model tests described later in the paper.

The type of vectoring nozzle chosen for a lift engine will be influenced strongly by the amount of vectoring required. Six vectorable lift nozzle concepts are shown in Fig. 2. Figure 2a features a rotating cascade which can operate through an angle of more than 90° from the engine centerline, or for lesser deflections in opposite directions. Figure 2b is a variant of Fig. 2a in which the rotating cascade has been replaced by a rotating elbow. Nozzles of types shown in Figs. 2a and 2b are relatively long for lift engines and their use may result in installation problems. Another difficulty can be the

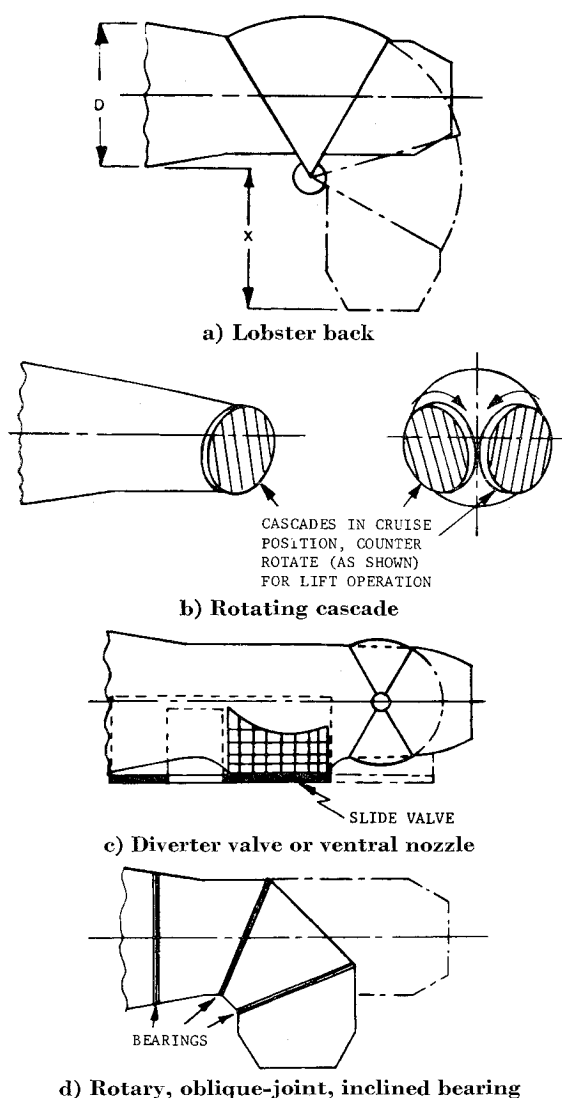


Fig. 3 Vectoring nozzles for lift/cruise engines.

generation of unwanted lateral forces during vectoring unless the lift engines are so grouped that these are cancelled out. The design in Fig. 2c utilizes moveable louvers as flow-deflection devices. The provision of a compensatory control device to adjust the louvers to maintain a constant effective exit area over the full range of vectoring is a complication.

A chute-type flow deflector is shown in Fig. 2d. Because a deflector of this type operates on the high-velocity exhaust efflux it will generally be large⁶ if satisfactory operation is to be obtained with appreciable flow-deflection angles. If the chute can be arranged to retract or to form part of the under-closure of the lift-engine bay it may still be regarded as a feasible technique for thrust vectoring.

Figure 2e shows a convergent nozzle fitted with a moveable end cap. This type is only suitable for deflecting the thrust axis approximately $\pm 30^\circ$ from the engine centerline. A logical development of such a design is Fig. 2f which is lighter and shorter than the Fig. 2e design and eliminates the inherent misalignment, in the vectored positions, of the centerbody with the nozzle exit. A compact nozzle of type in Fig. 2f is limited to a vectoring range of approximately $\pm 20^\circ$ from the centerline but this range may be increased when a multilayer, or a large-diameter, moveable cap is used.

Model tests were carried out to establish the performance of a simple hemispherical-plug, moveable-cap nozzle of the type shown in Fig. 2f. The test results are reported later.

Dual flow versions of the nozzle designs illustrated in Figs. 1 and 2 may be designed for use on nonmixed flow lift

turbofan engines. Several of these have been developed, some utilizing the Coanda effect for design simplification.

Nozzle Concepts for Lift/Cruise Engines

Four types of nozzles for lift/cruise applications are illustrated in Fig. 3. Each design is capable of deflecting the thrust axis at least 90° without producing net side forces at intermediate flow turning angles.

The "lobster-back" concept, Fig. 3a, is limited to installations with adequate ground clearance because X/D is large compared to the corresponding values for the other designs. The concept shown in Fig. 3b is a nozzle featuring twin, counter-rotating cascades set at compound angles. The cascades are largely hidden by the shadow of the engine cross section in the end view. This nozzle can be short and compact and is fairly simple as only two moving parts, the cascade rings, are employed. Its external shape may give rise to boat-tail fairing problems depending upon the manner of engine installation.

Figure 3c illustrates a diverter valve, or ventral, nozzle with clam-shell doors to shut off the cruise nozzle opening when operating in the lift mode. A slide valve, curved to conform to the engine cross section, controls flow through the cascade attached to an opening in the underside of the nozzle. The rigid cascade vanes can be installed such that a measure of flow deflection is provided which is controlled by translation of the slide valve. The geometry of a nozzle of this type allows the boat-tail surface to be well faired.

The concept in Fig. 3d is a compact, rotary, oblique-joint convergent nozzle with three bearings, two of which are inclined. The operation of the nozzle is apparent from inspection of the diagram. A rotary oblique-joint nozzle may be constructed with a minimum of one inclined bearing.

A convergent-divergent nozzle for operation at high forward flight Mach numbers can be fitted most easily to a diverter valve, similar to that illustrated in Fig. 3c, in place of a simple convergent nozzle. The substitution of twin convergent-divergent nozzles for the rotating cascades of Fig. 3b presents difficulties as the lift-mode downward projection parameter X/D becomes excessive. Divergent portions may be added to concepts of types Figs. 3a and 3d without reducing ground clearance in the lift mode, if they are permanently supported in the cruise position by rigid structures secured to nonmoving portions of the nozzle or the engine. The aerodynamic design of oblique-joint, convergent, vectoring nozzles is discussed later and experimental results are presented for such a nozzle having a single inclined bearing.

Lift-Engine Nozzle Performance

Short Annular Plug Nozzle

Model tests were carried out on a family of annular, convergent-passage, truncated plug nozzles covering a range of flow inclination angles. The objective was to establish data from which to select the shortest nozzle consistent with good performance. Figure 4 shows the family; the area ratio of each model is approximately 1.6.

To avoid subambient pressure on the end face of the truncated centerbody of a short annular nozzle, the exhaust

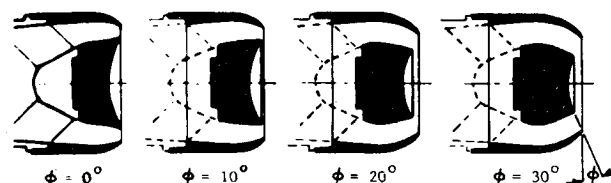


Fig. 4 Family of model convergent, annular, truncated plug nozzles.

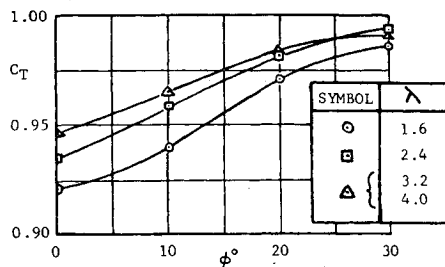


Fig. 5 Thrust coefficient vs throat inclination angle for four nozzle pressure ratios λ .

must flow slightly inward toward the center. The pressure gradient required to turn the jet efflux into an axial direction downstream of the nozzle exit causes a pressurization of the nozzle base region. Evacuation of the base area by a jet entrainment pumping action is inhibited, resulting in a high thrust coefficient. To minimize the axial length of a truncated plug nozzle it is desirable to limit the inclination angle of the gases leaving the nozzle exit to the minimum required to achieve a satisfactory thrust coefficient. This angle was found to be about 30° for the model configurations tested.

Experimental results are presented in Figs. 5-7 for four nozzle pressure ratios. Nozzle pressure ratio is defined as the total pressure measured at the approach to the nozzle divided by the surroundings (atmospheric) pressure P_∞ . The thrust coefficient (Fig. 5) increases with throat inclination angle ϕ . The maximum thrust coefficient occurred at an angle of about 30° . Discharge coefficient (Fig. 6) tends to decrease as ϕ increases. The discharge coefficient is based on the flow area of the throat formed between the lips of the shroud and plug.

Figure 7 shows the relationship between throat inclination angle and P_b/P_∞ , the area weighted mean static pressure recorded on the downstream face of the plug divided by the surroundings pressure. The mean base-pressure ratio starts to increase for inclination angles greater than approximately 10° . Base pressure increases rapidly with increasing nozzle pressure ratio at the higher inclination angles. This is due to the increase of throat Mach number with nozzle pressure ratio up to the critical value. For pressure ratios greater than critical, base pressure increases with nozzle pressure ratio as a result of the corresponding rise of throat static pressure.

It was found that the dimensionless axial length X/D (see Fig. 1a) of a full-size nozzle design based on the optimum model configuration with the 30° inclination angle was less than 0.2.

Simple Vectoring Nozzle

Figure 8 is an illustration of a model which has been tested to establish the performance of a short, simple, vectoring

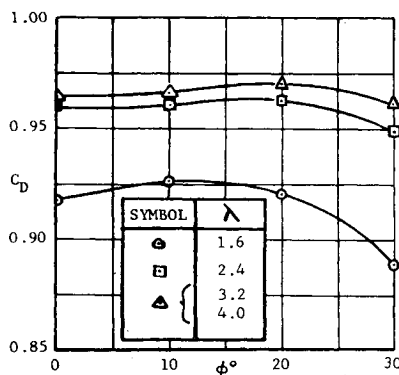


Fig. 6 Discharge coefficient vs throat inclination angle for four nozzle pressure ratios λ .

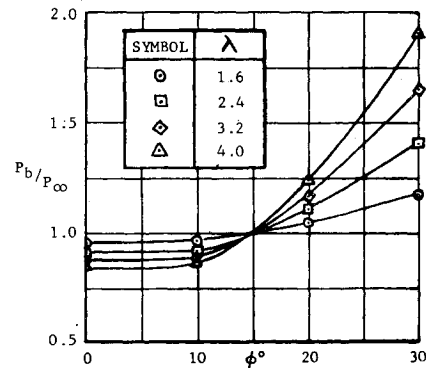


Fig. 7 Area weighted base pressure ratio vs throat inclination angle for four nozzle pressure ratios λ .

nozzle similar to that shown in Fig. 2f. The full-scale nozzle consists of an inner hemispherical body, functioning as the fairing of the downstream face of the engine turbine, held in place by flow-straightening struts secured to an outer, approximately hemispherical, shell forming an extension of the engine's outer casing. An external moveable hemispherical cap is constrained to fit closely over the curved portion of the engine casing. Gases leaving the nozzle pass through a large circular hole cut in the end of the curved portion of the engine case; a smaller hole in the movable outer cap forms the nozzle discharge orifice. Thrust vectoring, up to a maximum of approximately $\pm 20^\circ$ from the engine centerline, is obtained by moving the outer cap such that the discharge orifice is aligned in the appropriate direction.

The contracting passage formed by the space between the inner and outer surfaces of the nozzle carries the flow around to the throat, which lies on a conical surface connecting the periphery of the exit with the centerbody; the gases then turn and leave the nozzle through the exit in the moveable cap. The flow separation off the centerbody surface and the flow straightening, occurring partly external to the nozzle, have been found, from the model tests, to be stable at all operating conditions.

It has been found that a full-size hemispherical nozzle, of the type described, capable of vectoring to a maximum of $\pm 20^\circ$ from the engine centerline, can be designed with a dimensionless length X/D (see Fig. 2a) less than 0.3.

The performance of a vectorable lift nozzle, predicted from the results of tests carried out on the model illustrated in Fig. 8, is shown in Figs. 9 and 10. The model has an area ratio of approximately 1.6. The upper portion of Fig. 9 presents the resultant thrust coefficient, acting in the direction (β) to which the flow had been deflected, for three prescribed values of the geometric angle β_0 . Since the data lie within the range $0.984 \leq C_T \leq 0.991$, the nozzle internal performance is substantially unaffected by vectoring and only slightly effected by nozzle pressure ratio over the range investigated.

The nozzle discharge coefficients based on the area of the conical throat formed between the lip of the exit and the surface of the plug are also shown in Fig. 9. The relatively low values are due to the strong vena-contracta effect resulting from the nozzle flow passage geometry. This factor also accounts for the dependence of C_D on pressure ratio even at pressure ratios much greater than the critical value.

The upper portion of Fig. 10 shows the actual gas turning angle β plotted against nozzle pressure ratio. Each curve corresponds to a particular value of the nominal flow vector



Fig. 8 Model vectorable lift-engine nozzle.

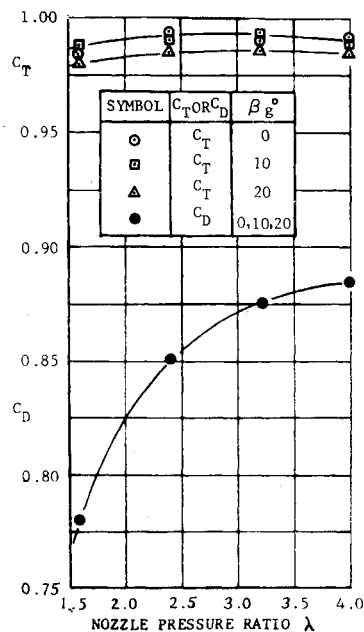


Fig. 9 Thrust and discharge coefficients vs nozzle pressure ratio.

angle β_g based on the nozzle's geometric setting. With $\beta_g = 20^\circ$ the actual flow deflection β is approximately 18° . When $\beta_g = 10^\circ$, β is between 9° and 10° . At zero nominal deflection $\beta \approx \beta_g$. The lower portion of Fig. 10 shows the lateral displacement, Δr , of the thrust vector as a fraction of the radius r_{EXT} of the nozzle exit. The value of $\Delta r/r_{EXT}$ is always less than 0.04. The actual gas turning angle β and Δr were deduced from results obtained with a multicomponent force balance.

Effect of Whirl on Thrust Coefficient

It is particularly important that nozzles for lift engines should not only be of minimum axial length but should also be of very light weight. Cost of manufacture is another factor which must be taken into account when deciding upon an optimum nozzle design. The omission of flow-straightening vanes downstream of the turbine is one way in which nozzle weight may be minimized and construction costs lessened. Three or four struts may be adequate to retain the nozzle centerbody but will not also serve as flow-straightening vanes unless their chord is large, probably larger than permissible within the compass of the restricted axial length of the designs previously described. The tests on the model non-vectoring annular plug and vectoring hemispherical nozzles were performed with pure axial flow approaching the nozzle. A theoretical analysis has, therefore, been carried out to establish the approximate effect on thrust coefficient of a whirl component in the flow entering the nozzle. An indication was obtained by this means of the performance penalties resulting from elimination of flow-straightening vanes at the entrance to the nozzle as a function of turbine residual whirl.

The analysis is based on continuity of mass flow and conservation of angular momentum, which are each equated at upstream and downstream stations (labeled 1 and 2, respectively on Fig. 11). It is assumed that, apart from whirl, flow is parallel to the engine centerline. Conservation of angular momentum between stations 1 and 2 implies that internal skin friction and also mixing of the nozzle exhaust with air from the surroundings between the exit of the nozzle and station 2 are both negligible. Other assumptions are:

- 1) Whirl is of the free vortex type in the annular duct at station 1.
- 2) Total head pressure at station 1 is uniform across the annulus.

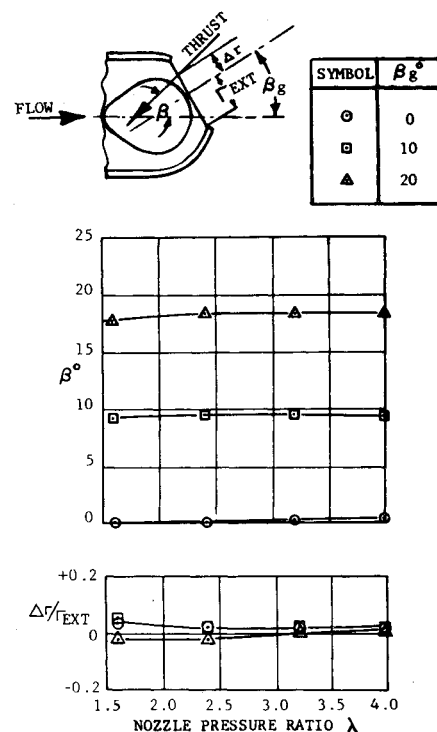


Fig. 10 Actual flow deflection and displacement of thrust axis vs nozzle pressure ratio.

- 3) The axial velocity component is uniform across station 2.

4) Free vortex flow prevails over the outer half of the radius of the jet (station 2); whirl is of the forced vortex type between the engine centerline and half the radius of the jet. Pressure and velocity match at the interface between the free and forced vortex flows.

- 5) Density is constant across station 1 and across station 2. The reduction in density between stations 1 and 2 is allowed for in the normal manner for compressible flow.

It may be pointed out that assumptions 3, 4, and 5 are not so restrictive as, on first consideration, may appear to be the case. Only 25% of the jet efflux passes between the engine centerline and half the radius of the jet; hence detail assumptions about the core of the vortex at station 2 have a relatively minor effect on the final results of the analysis.

Figure 12 shows the theoretically determined variation of thrust coefficient (C_T) with whirl angle for a ratio of the inner to outer radii of the turbine exhaust annulus of 0.7 and a nozzle pressure ratio of 2.5. The whirl angle and the turbine outlet Mach number $M_{(RESUL)1}$ are those prevailing at the mean height of the turbine blades at station 1. Curves are shown for a range of values $M_{(RESUL)1}$ from 0.3 to 0.6. It was as-

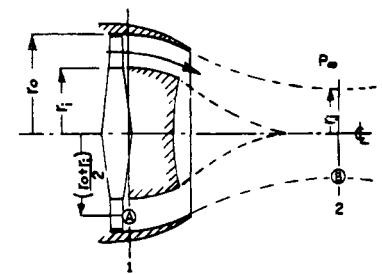
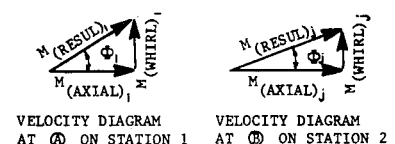


Fig. 11 Nozzle geometry and notation for analysis of effect of whirl on thrust coefficient.



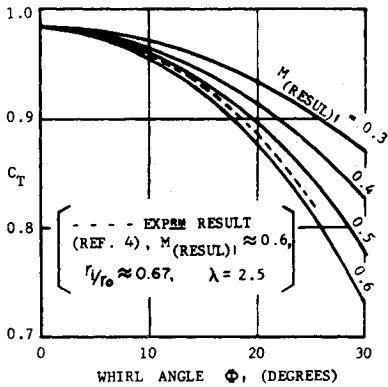


Fig. 12 Predicted effect of whirl on thrust coefficient. $r_i/r_o = 0.7$, nozzle pressure ratio $\lambda = 2.5$.

sumed that without whirl the nozzle thrust coefficient is 0.985, the thrust coefficients are based upon the full total pressure of the turbine exhaust. An experimental result,⁴ modified to this form of presentation, is shown dotted on Fig. 12. Figure 13 displays the significance of turbine exhaust annulus proportions on the thrust loss due to whirl. As the ratio r_i/r_o approaches unity, whirl-induced losses increase because of the effect of the conservation of angular momentum. The opposite effect accounts, in part, for the relationship between nozzle pressure ratio and thrust coefficient shown in Fig. 14. As nozzle pressure ratio increases, the thrust and jet diameter also increase, thereby lessening the importance of whirl at the nozzle entry.

It may thus be concluded that even modest turbine residual whirl can, for conditions typical of those applicable to lift-engine nozzles, have a serious deleterious effect on thrust coefficient and should, in general, be eliminated from flow entering such a nozzle.

Nozzle for Lift/Cruise Applications

Nozzle Design

Of the concepts reviewed, a design similar in principle to that shown in Fig. 3d was selected for further development.

An oblique-joint vectoring nozzle was chosen in preference to other types because

- 1) The thrust vector remains on a vertical plane during transition.
- 2) Application of thrust during transition is continuous over the full range of vectoring.
- 3) The internal gas passage is, in essence, unimpaired in the cruise position being similar to that of an orthodox, non-vectoring, convergent nozzle.
- 4) The installational characteristics are, in general, acceptable.

- A two bearing design was chosen because
- 5) There are only two major moving parts.
- 6) Projection towards the ground in the lift mode is less than for a three, or more, bearing version. Generally, as a consequence of the finite thickness of a bearing assembly, pro-

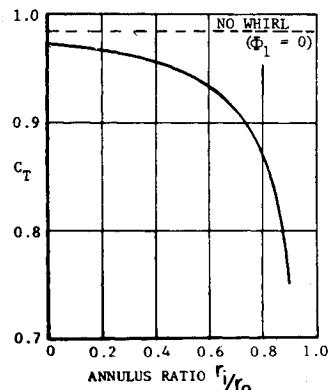


Fig. 13 Predicted effect of annulus ratio on thrust coefficient with whirl. $M_{(resul)1} = 0.4$, $\Phi_1 = 20^\circ$, nozzle pressure ratio $\lambda = 2.5$.

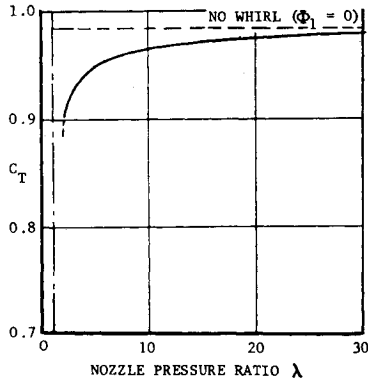
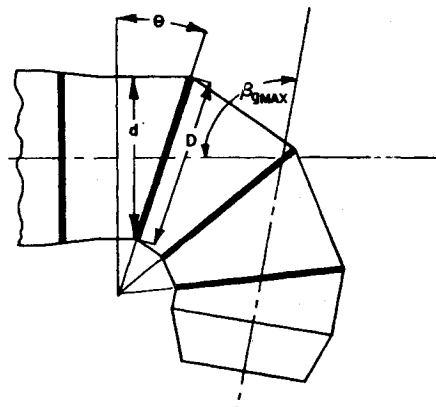


Fig. 14 Predicted effect of nozzle pressure ratio on thrust coefficient with whirl. $M_{(resul)1} = 0.4$, $\Phi_1 = 20^\circ$, $r_i/r_o = 0.7$.

jection towards the ground increases in proportion to the number of oblique joints.

An argument against the use of a small number of oblique joints is the magnitude of the departure from a circular cross section in the nozzle approach duct. Elliptic ducts require more structural reinforcement than those of circular cross section. Also, for a prescribed flow area, the smaller the number of oblique joints, the larger is their diameter. The table in Fig. 15 shows the ratio of minor to major diameters of the nozzle approach duct vs the number of angled joints for 100° maximum deflection. The ratio of the major diameter of the elliptic-section nozzle approach duct to the diameter of a circular cross section of the same flow area is also given. Nozzle length can be reduced by using an elliptic cross section exit. This eliminates the need for an elliptic-to-circular transition piece downstream of the last bearing. An important benefit derived from this is, therefore, minimization of the projection towards the ground of the lift configuration. For these reasons there does not, in general, appear to be a great difference between the estimated specific weights of full-scale, oblique-joint, vectoring nozzles with either one or two inclined bearings.

The installation of an oblique-joint vectoring nozzle can be simplified if the engine cowling, or fairing, is attached directly to the moving parts of the nozzle. The nonmovable cowling attached to the aircraft therefore terminates at the plane of the



$$\theta = \frac{\beta_{g \text{ MAX}}}{2n} \quad , \quad \frac{d}{D} = \cos \theta \quad , \quad \frac{D}{d_{\text{EQV}}} = \sqrt{\sec \theta}$$

FOR $\beta_{g \text{ MAX}} = 100^\circ$;

n	d/D	D/d _{EQV}
1	0.643	1.248
2	0.906	1.050
3	0.958	1.020
4	0.976	1.011

Fig. 15 Relationship between the number of bearings and the proportions of oblique-joint vectoring nozzles.

bearing at the upstream end of the nozzle. An arrangement of this type eliminates the need for a cutout, and consequently a closure, in the underside of the fuselage or engine nacelle.

If the vectoring nozzle is to be used on a turbofan engine a decision must be made whether to 1) bring the fan and gas generator flows into contact with each other at the upstream end of the nozzle without provision of a flow mixer as such; 2) premix the fan and gas generator flows at the upstream end of the nozzle; or 3) construct the nozzle with coaxial passages to keep the fan and gas generator flows separated up to the nozzle exit plane. These three possibilities are considered in the following section and it is shown that the second technique is usually to be preferred.

Flow Turning in the Lift Mode

The behavior of a homogeneous, uniform, stream flowing through a circular-section duct containing a sharp bend, or elbow, is fairly well understood. Generally, the separation and turning losses can be held to acceptable values by proper design.

Coaxial flows in direct contact will, however, behave differently in a bend unless certain specific conditions are satisfied. Figure 16 illustrates coaxial flow from a turbofan engine turning through a nozzle in the lift configuration. Because the fan and gas generator flows are only brought into contact at entry to the nozzle it may be assumed that negligible mixing of the two flows occurs upstream of the bend. An analysis of this type of coaxial flow, summarized in the right-hand portion of Fig. 16, leads to an expression for the radii of curvature of streamlines in fluids 1 and 2 when each is subjected to the same radial pressure gradient at the same static pressure level:

$$r_2/r_1 = (\gamma_2/\gamma_1)(M_2/M_1)^2$$

This equation indicates that when the Mach number (M_2) of the gas generator flow exceeds the corresponding fan flow Mach number M_1 , the gas generator flow will tend to impinge on the outer surface of the bend. If $M_1 > M_2$ the gas generator flow will, conversely, tend to turn more sharply than the fan flow and become displaced toward the inside of the elbow. It can be anticipated that either situation, but especially the case in which $M_2 > M_1$, results in the generation of severe turbulence with attendant losses. Tests with small-scale models substantiate these conclusions.

It therefore appears that, unless $M_1 = M_2$, turning the fan and gas generator flows of a turbofan engine without significant losses involves either premixing upstream of the nozzle or, alternatively, conducting the fan and gas generator flows in separate, possibly coaxial, channels to or near the nozzle exit. Premixing the fan and gas generator flows upstream of the exhaust nozzle can produce a slight augmentation effect as indicated in the next section.

Effect of Flow Mixing on Thrust

The effects of mixing on thrust were studied theoretically since data available in the literature⁷ were not sufficiently

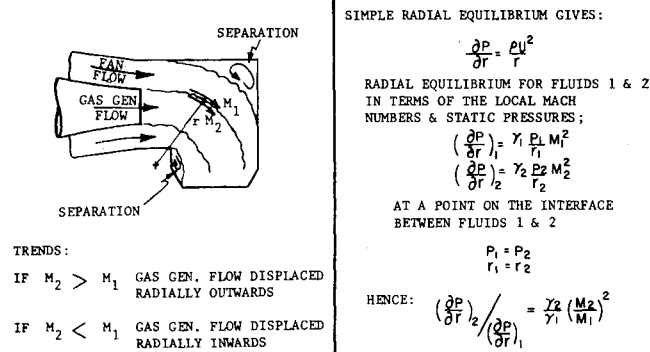


Fig. 16 Behavior of a coaxial flow system in a bend.

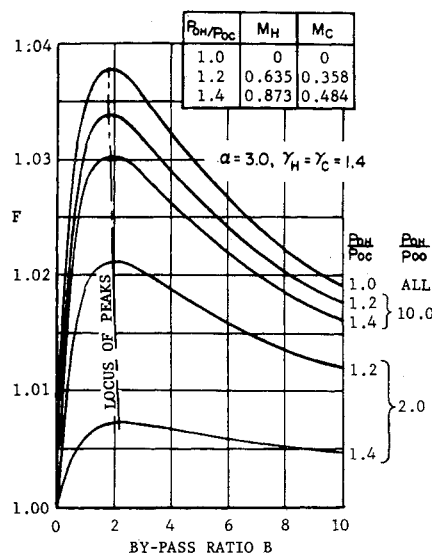


Fig. 17 Maximum potential thrust augmentation due to mixing, $P_{oH}/P_{oc} \geq 1.0$.

comprehensive to permit estimates to be made over a wide range of engine operating conditions. The analysis was based upon the application of continuity, momentum and energy equations. Because mixing was assumed to be complete, assumptions related to the velocity profile prevailing during mixing were not required. Also the mixing tube was assumed to be of constant cross-sectional area throughout its length or, alternatively, the cross-sectional area was adjusted such as to maintain a uniform static pressure everywhere within it.

The theoretical analysis was arranged in such a way that the mixing conditions giving maximum thrust augmentation could be established for prescribed engine bypass ratio, fan and gas generator nozzle pressure ratios. The thrust augmentation ratio F due to mixing was defined to be the ideal thrust obtainable from the fully mixed flow divided by the sum of the ideal thrusts of the fan and gas generator flows had each been expanded isentropically through separate nozzles. Hence it may be shown that

$$F = \frac{\left[(1+B)(\alpha+B) \left\{ 1 - \left(\frac{P_{\infty}}{P_{oM}} \right)^{(\gamma_M-1)/\gamma_M} \right\} \right]^{1/2}}{\left[\alpha \left\{ 1 - \left(\frac{P_{\infty}}{P_{oH}} \right)^{(\gamma_H-1)/\gamma_H} \right\} \right]^{1/2} + B \left[1 - \left(\frac{P_{\infty}}{P_{oc}} \right)^{(\gamma_C-1)/\gamma_C} \right]^{1/2}}$$

It was found from the study that for the conditions pertaining to maximum thrust augmentation there was no difference between the results obtained on the basis of either a constant-area mixing tube or a uniform static pressure within the mixing tube. It emerged, therefore, that the optimum mixing conditions corresponded, at least for idealized cases, to a uniform static pressure within a mixing tube of constant cross-sectional area.

Theoretical results are shown in Figs. 17-19 plotted over a range of bypass ratios from 0 to 10. It may be seen from these three figures that the bypass ratio corresponding to peak thrust augmentation due to mixing lies approximately in the range from $1\frac{1}{2}$ to $2\frac{1}{2}$ for the flow conditions considered. Also, the maximum theoretical thrust gain increases rapidly as the gas generator to fan flow enthalpy ratio α increases.

Naturally, the effects of incomplete mixing and also of losses due to wall friction drag in the mixer itself will tend to detract from the potentially beneficial effects of mixing the fan and gas generator streams of a turbofan engine. For example, with an enthalpy ratio of 3, a bypass ratio of 2, $P_{oH}/P_{oc} = 1.2$ and a gas generator nozzle pressure ratio of 2:1 the potential thrust

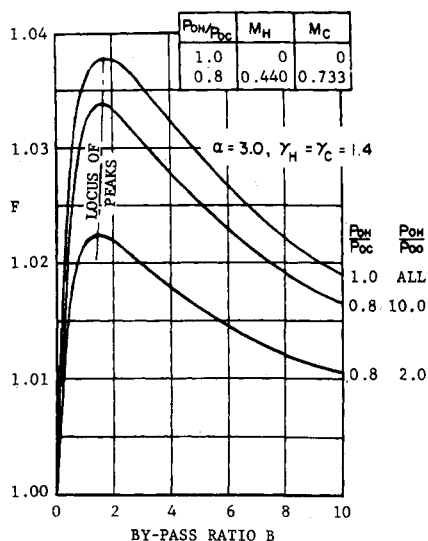


Fig. 18 Maximum potential thrust augmentation due to mixing, $P_{oH}/P_{oc} \leq 1.0$.

augmentation ratio of 1.021 resulting from full mixing will be reduced to approximately unity by losses of total pressure of about 1.6% in each of the flows entering the mixer with a total pressure loss of similar magnitude occurring in the mixed stream. With a gas generator nozzle pressure ratio of 10:1 losses of approximately 10% in each flow will be required to completely negate the potential thrust augmentation ratio of 1.034 corresponding to $P_{oH}/P_{oc} = 1.2$.

It can be seen, therefore, that in general little or no gain in thrust can be expected from the addition of a mixer upstream of the nozzle of a turbofan engine for conditions representative of static operation at sea level. An increase in thrust may, however, be obtainable at the higher pressure ratios existing under flight conditions. It follows that serious consideration should be given to the installation of flow mixers in vectored thrust turbofan engines in preference to alternative configurations incorporating separate fan and gas generator nozzles.

Performance with Mixed Flow

Model tests were carried out to establish the static performance of an oblique-joint nozzle of the single inclined bearing type. The model was tested with a uniform, homogenous,

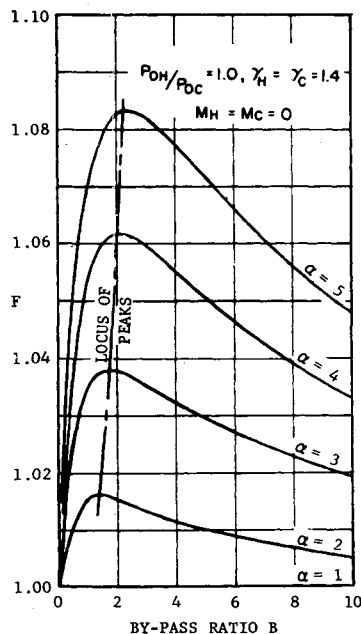


Fig. 19 Effect of enthalpy ratio on potential thrust augmentation.

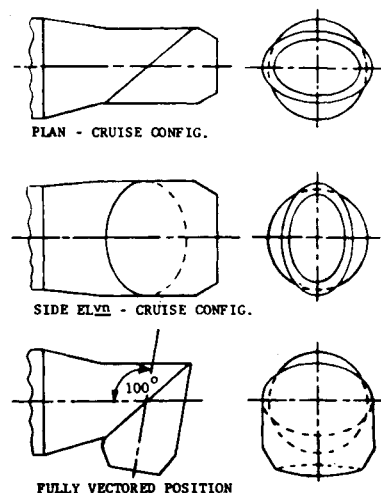


Fig. 20 Sketch showing aerodynamic design of model vectored nozzle.

supply of cold compressed air as the working fluid. The aerodynamic design of the model is illustrated in Fig. 20 which shows the nozzle in both the cruise and fully vectored (100° flow deflection) modes. The area ratio is approximately 2.0.

Performance of the model is displayed in Fig. 21 for zero and 100° nominal flow deflections. Both the thrust and discharge coefficients are between 3 and 5% lower in the fully vectored position than for the cruise geometry. The cruise thrust coefficient was comparable with that obtainable from a simple convergent nozzle of circular cross section.

A flow visualization study revealed strong secondary flows in the lift configuration, separation from the inside of the bend was also observed. A modification (to inhibit the secondary flows) was made by adding filling material between the oblique joint and the nozzle exit in the region of the major axis of the elliptic section. Figure 22 shows the modification and the performance obtained. The cruise thrust coefficient was substantially unaffected by the change but in the fully vectored position, thrust was increased as were the discharge coefficients in both modes of operation. The thrust and discharge coefficients in the fully vectored configuration were found to be between 2 and 3% lower than the corresponding values with zero flow deflection.

A further modification, the addition of filling material upstream of, and in, the plane of the nozzle exit in the neighbourhood of the minor axis of the elliptic section was superimposed on the modification previously described. The purpose of the added material was to fill up the region of flow separation occurring on the inside of the bend under simulated lift conditions. A corresponding filling was also added to the outer surface of the bend in order to preserve the symmetry of the nozzle in the cruise mode. The modification and the performance obtained with the fully modified nozzle are shown in Fig. 23. The thrust coefficients are substantially similar, for lift and cruise operation, to those shown in Fig. 22. The discharge coefficients in both the lift and cruise configurations were found to be approximately identical.

The reason for the lack of dependence of the discharge coefficient on the vector setting of the fully modified nozzle is, apparently, due to the effect of the pressure loss engendered by vectored operation being offset by a reduction of jet contraction (vena-contracta effect) downstream of the nozzle exit. The vena-contracta is dependent upon the flow field approaching the nozzle exit as well as on the geometry of the physical boundaries containing the flow system. It is important that, for the satisfactory operation of a vectored nozzle, the discharge coefficient should be approximately the same in both the lift and cruise modes if no provision is made to vary nozzle exit area in a compensatory manner.

It was found from the model tests that between 1½° and 2° of overturning of the flow occurred at the fully vectored setting of each of the configurations investigated. In the cruise

Fig. 21 Performance of model vectoring nozzle prior to modification.

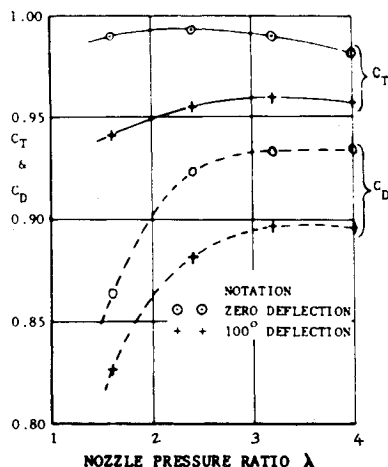
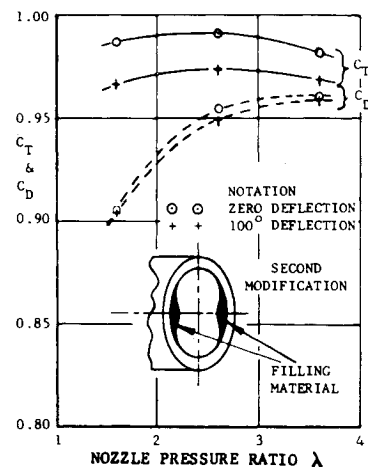


Fig. 23 Performance of model vectoring nozzle with the first and second modifications incorporated.



modes the thrust axes aligned nearly exactly with the centerline of the nozzle in every case.

Conclusions

Nozzles of the annular, truncated plug type are particularly suitable for lift engine applications when thrust vectoring is not a requirement. Model tests show that nozzles of this kind may be designed with a very short axial length without sacrifice of performance.

A satisfactory, simple, type of vectorable nozzle for use on lift engines is the hemispherical cap and centerbody design. Such a nozzle may be arranged to deflect the thrust axis up to approximately 20° from the engine centerline in any direction. The results of model tests confirm that a high thrust coefficient is obtainable and that the thrust and discharge coefficients are insensitive to vectoring.

It is not generally desirable to lighten, to shorten, or to cheapen lift-engine nozzles by omitting flow-straightening devices as the resultant loss of thrust can be very serious, more than sufficient to negate the advantage, unless turbine residual whirl is extremely small.

It is possible to construct satisfactory nozzles for lift/cruise applications in several ways. Types which appear to hold

particular promise are the ventral, or diverter valve, nozzle and the inclined bearing oblique-joint vectoring nozzle concepts. Optimum configurations for inclined bearing, oblique-joint, vectoring nozzles appear to be those having either one or two inclined bearings. Generally, designs with one inclined bearing are mechanically more simple than those with two such bearings but are slightly more difficult to install because of their elliptic cross section. When a vectoring nozzle is used on a turbofan engine the fan and gas generator flows should, in the interests of maximizing thrust in the lift mode, be either mixed upstream of the nozzle or discharged through separate exits. The first solution appears to be the most attractive from an engine performance standpoint. It has been demonstrated, from model tests, that a simple single inclined joint vectoring nozzle is capable of attaining satisfactory internal performance in both the lift and cruise modes when supplied with a homogeneous flow representing the exhaust efflux of a turbojet or the mixed fan and gas generator flows of a turbofan engine.

References

- ¹ Spreeman, K. P. and Sherman, I. R., "Effects of ground proximity on the thrust of a simple downward-directed jet beneath a flat surface," NACA TN 4407 (1958).
- ² Vogler, R. D., "Ground effects on single and multiple-jet VTOL models at transition speeds over stationary and moving ground planes," NASA TN-D-3213 (1966).
- ³ Higgins, C. C., Kelly, D. P., and Wainwright, T. W., "Exhaust jet wake and thrust characteristics of several nozzles designed for VTOL downwash suppression," NASA CR-373 (1966).
- ⁴ Baker, V. D., Johnson, R. A., Brasket, R. G., and Lamb, O. P., "Experimental results with lift engine exhaust nozzles," AIAA Paper 65-574 (1965).
- ⁵ Goodson, W. and Otis, J. H., Jr., "Effect of ratio of jet area to total area and of pressure ratio on lift augmentation of annular jets in ground effect under static conditions," NASA TN-D-720 (1961).
- ⁶ McArdle, J. G., "Internal characteristics and performance of several jet deflectors at primary-nozzle pressure ratios up to 3.0," NACA TN 4264 (1958).
- ⁷ Seddon, J. and Dyke, M., "Ejectors and mixing of streams," Ministry of Aviation, Royal Aircraft Establishment Library Bibliography No. 252 (1964).

Fig. 22 Performance of model vectoring nozzle after first modification.

